Acta Crystallographica Section D
Biological Crystallography
ISSN 0907-4449

Structure of a phosphoglycerate mutase:3-phosphoglyceric acid complex at 1.7 Å

Gina S. Crowhurst,[a] Andrew R. Dalby,[a] Michail N. Isupov,[a] John W. Campbell[b] and Jennifer A. Littlechild[a]*

[a]Schools of Chemistry and Biological Sciences, University of Exeter, Stocker Road, Exeter, Devon EX4 4QD, England, and [b]Daresbury Laboratory, Daresbury, Warrington, Cheshire WA4 4AD, England

Correspondence e-mail: j.a.littlechild@ex.ac.uk

Received 21 May 1999
Accepted 21 July 1999

PDB Reference: phosphoglycerate mutase:3-phosphoglyceric acid complex, 1qhf.

The crystal structure of the tetrameric glycolytic enzyme phosphoglycerate mutase from the yeast *Saccharomyces cerevisiae* has been determined to 1.7 Å resolution in complex with the sugar substrate. The difference map indicates that 3-phosphoglycerate is bound at the base of a 12 Å cleft, positioning C2 of the substrate within 3.5 Å of the primary catalytic residue, histidine 8.

1. Introduction

Saccharomyces cerevisiae phosphoglycerate mutase (*Sc*PGM) is a homotetrameric enzyme with a subunit M_r of 27 kDa which reversibly catalyzes the transfer of a phosphate group from C3 of 3-phosphoglycerate (3PG) to C2 of 2-phosphoglycerate (2PG; Fothergill-Gilmore & Watson, 1989). The structure of *Sc*PGM was originally solved at 3.5 Å resolution (Campbell *et al.*, 1974). Further studies at 2.8 Å (Winn *et al.*, 1981) positioned 3PG in the active site; however, this resolution did not allow accurate placement of the active-site residues, notably of the two active-site histidines His8 and His181. The structure of native *Sc*PGM has been described to 2.3 Å resolution and the errors in the sequence corrected (Rigden *et al.*, 1998). The 2.3 Å structure was solved in a different, although related, space group from that described here and did not contain the enzyme substrate. More recently, a 2.12 Å structure has been solved, again in a different space group (Rigden *et al.*, 1999).

For *Sc*PGM to be catalytically competent His8 must be phosphorylated, which requires trace amounts of the cofactor 2,3-bisphosphoglycerate (2,3-BPG) to be present *in vivo* (Nairn *et al.*, 1995). Site-directed mutagenesis has shown that replacing either of the active-site histidines (His8 and His181) with alanine dramatically reduces *Sc*PGM isomerase activity by preventing the formation of the phosphohistidine moiety (White & Fothergill-Gilmore, 1992). Mutation of important active-site residues Ser11, Glu15, Gly21, Ala60 and Arg87 changes the affinity and specificity of *Sc*PGM for 3PG (Ravel *et al.*, 1996).

Close to the active-site entrance lies the C-terminal region of approximately 14 residues, whose atomic coordinates have not been included in any of the five structures deposited in the Protein Data Bank (Bernstein *et al.*, 1977; PDB codes 3pgm, 1bq3, 1bq4, 4pgm and 5pgm), since its presumed high flexibility leads to poorly defined electron density. This C-terminal structure appears to be crucial in the reaction mechanism for regulating substrate release and providing a suitable environment for phosphate transfer, since mutations in this region reduce catalytic activity (Garel *et al.*, 1989). The *Sc*PGM structure presented in this paper allows accurate positioning

Table 1
Statistics of the Ramachandran plot of the finished model.

Data obtained using *PROCHECK* (Laskowski *et al.*, 1993).

Residues in most favoured regions (A, B, L)	377	90.2%
Residues in additionally allowed regions (a, b, l, p)	39	9.3%
Residues in generously allowed regions (~a, ~b, ~l, ~p)	0	0.0%
Residues in disallowed regions	2	0.5%

of 3PG in the active site and provides structural information to 1.7 Å resolution.

2. Experimental

*Sc*PGM was purified from bakers' yeast by a modification of the method described by Winn *et al.* (1981). Bakers' yeast, *S. cerevisiae*, was broken by grinding with acid-washed beads, resuspended in buffer containing 20 m*M* Tris–HCl pH 7.0 and clarified before adding ammonium sulfate (enzyme grade) to 30%. After centrifugation, ammonium sulfate was added to the supernatant to a final concentration of 75%. The resultant pellet was resuspended in 20 m*M* Tris–HCl pH 7.0 and dialysed against this buffer. Cation-exchange chromatography was performed using CM cellulose (Whatman) in Tris–HCl buffer at pH 7.0 with a 0.1–1.0 *M* NaCl gradient. A final gel-filtration step using Superose 12 (Pharmacia) in 20 m*M* Tris–HCl pH 7.0, 5% ammonium sulfate resulted in protein of sufficient purity for crystallization trials. All operations were carried out at 277 K. Crystals of *Sc*PGM were grown from 55% ammonium sulfate in 10 m*M* imidazole buffer pH 6.8 in the presence of 1 m*M* 3PG substrate using the hanging-drop technique at 277 K. The concentration of protein used was 10 mg ml^{-1}. Crystals were harvested into a mother liquor composed of 65% ammonium sulfate, 10 m*M* imidazole buffer pH 6.8 and 1 m*M* 3PG and were stored at 277 K until use. X-ray diffraction data were collected at room temperature to 1.7 Å on beamline 9.6 at the Daresbury Synchrotron source using a MAR Research image-plate detector. Data were processed in space group *C*2 using *DENZO* and *SCALEPACK* (Otwinowski & Minor, 1997), with resultant unit-cell parameters a = 96.15, b = 85.8, c = 81.9 Å, β = 120.5°.

A total of 95 787 measured reflections were merged to give 42 944 unique reflections to 1.7 Å. To increase the completeness at low resolution, 'in-house' 2.8 Å data collected on a Siemens multiwire detector with Cu $K\alpha$ radiation (Winn *et al.*, 1981) were scaled and merged with the synchrotron data with an overall merging R factor of 8.9% using *BLANC* (Vagin *et al.*, 1998). A total of 3754 reflections were added to give 96.5% completeness to 3.3 Å (cumulative completeness of 82.5 to 1.7 Å; Fig. 1). Refinement of the *Sc*PGM starting model was carried out using *REFMAC* (Murshudov *et al.*, 1997) on 44 341 reflections with anisotropic data correction. The 3PG substrate coordinates were obtained from the Cambridge Crystallographic Data Centre (Allen, 1998). After inclusion of the substrate, further refinement was carried out using occupancies of 0.4 for 3PG and 0.6 for the overlaid sulfate molecule. To determine these figures, the occupancies were adjusted until the B factors for the phosphate and overlaid sulfate moiety were comparable with the B factors of the remaining constituent atoms of the sugar substrate moiety. The model was rebuilt in *O* (Jones *et al.*, 1991) using both $2F_o - F_c$ and $F_o - F_c$ difference maps. Water molecules were added using *ARP* (Lamzin & Wilson, 1993). 3PG and sulfate molecules were added where the electron density suggested their inclusion.

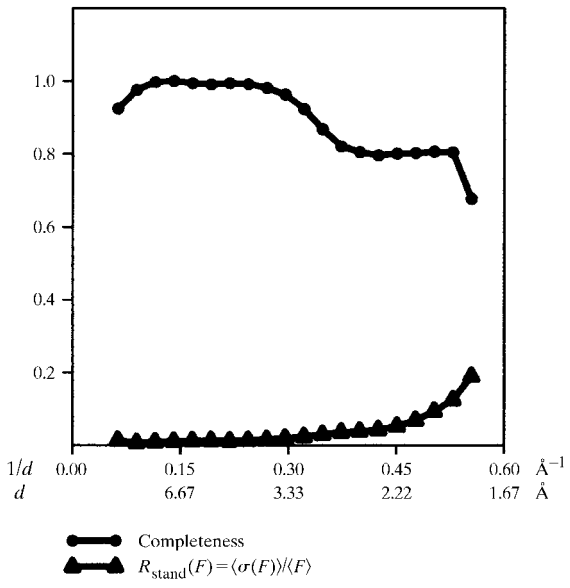

Figure 1
Completeness of data and $R_{standard}$ of data plotted *versus* resolution. The figure was prepared using *SFCHECK* (Vaguine *et al.*, 1999).

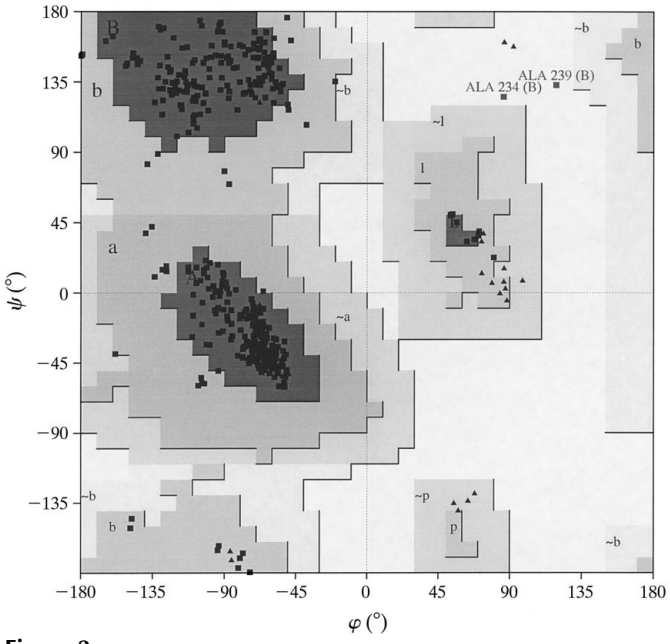

Figure 2
The Ramachandran (φ, ψ) plot for the two crystallographically independent subunits of *Sc*PGM. Glycine residues are represented as triangles and all other residues are represented as squares. Residues 1–240 have been included. Figure prepared using *PROCHECK* (Laskowski *et al.*, 1993).

Table 2
A summary of refinement statistics of phosphoglycerate mutase.

Space group	*C*2
Unit-cell parameters (Å,°)	a = 96.15, b = 85.80, c = 81.90, β = 120.54
R_{sym}† (%)	8.8
Multiplicity	2.2
Completeness of data (cumulative) (%)	82.5
Completeness of data (2.3–1.7 Å) (%)	77.2
Resolution range (of input data) (Å)	19.9–1.76
Number of atoms	4097
Number of residues (per subunit)	240
Number of water molecules	267
Number of sulfate molecules (per subunit)	1 at occupancy 1.0, 1 at occupancy 0.6
Number of substrate molecules (per subunit)	1 at occupancy 0.4
Percentage solvent	51.1
R‡ (%)	17.7
R_{free}§ (5% total data) (%)	21.5
Average B factor for atomic model (Å^2)	26.8
Average B factor for protein atoms (Å^2)	25.7
Average B factor for water atoms (Å^2)	38.0
R.m.s. deviations from ideality (target values in parentheses)	
Bond lengths (Å)	0.012 (0.02)
Bond angles (Å)	0.029 (0.04)
I-4 neighbours (Å)	0.034 (0.05)
Planar groups (Å)	0.02 (0.02)
Chiral volumes (Å^3)	0.15 (0.15)
Torsion angles (°)	
Planar	4.0 (7.00)
Staggered	15.0 (15.00)
Orthonormal	29.2 (20.00)
B-factor correlation (Å^2)	
Main-chain bond	2.8 (4.0)
Main-chain angle	3.5 (6.0)
Side-chain bond	5.7 (8.0)
Side-chain angle	7.7 (10.0)

† $R_{sym} = \sum_h \sum I|\langle I_h\rangle - I(h)I| / \sum_h \sum I(h)I$, where $I(h)$ is the intensity of the reflection h, $\sum_h$ is the sum over all the reflections and $\sum I$ is the sum over I measurements of the reflection. ‡ $R = \sum ||F_o| - |F_c|| / \sum |F_o|$. § R_{free} is as defined by Brünger (1992).

Table 3
A brief description of the B factors of the 3PG substrate and of the sulfate anions described in the text.

Occupancy can be assumed to be 1.0 unless stated otherwise. The values described are an average of the B factors of the atoms in the species mentioned.

Subunit *A*	
3PG phosphate moiety†	42.9
3PG sugar (3C) moiety†	37.6
Overlaid sulfate anion‡	27.4
Sulfate anion	69.6
Subunit *B*	
3PG phosphate moiety†	44.2
3PG sugar (3C) moiety†	40.3
Overlaid sulfate anion‡	31.7
Sulfate anion	69.7

† Occupancy of 0.4. ‡ Occupancy of 0.6.

3. Results and discussion

The model of *Sc*PGM was refined to an R factor of 17.7% (R_{free} of 21.5%). The refined model contains two *Sc*PGM subunits, two 3PG molecules (40% occupancy), 266 waters, two sulfate groups with 100% occupancy and two sulfate groups with 60% occupancy per asymmetric unit. Table 1 provides information on the quality of the structure. Over 90% of residues are in the most favoured regions of the Ramachandran plot, as expected for a good-quality model (Fig. 2). Table 2 outlines the refinement statistics. The two residues located in the disallowed region (Ala234 and Ala239) are positioned in the flexible C-terminal loop of the *B* subunit.

The $2F_o - F_c$ and $F_o - F_c$ difference maps showed the presence of electron density corresponding to the shape of a phosphate group, with additional electron density extending in the direction of residue 207. Fig. 3 shows the 3PG substrate with an occupancy of zero superimposed on the $F_o - F_c$ difference map. The 3PG molecule was fitted into this electron density with the phosphate moiety occupying density previously assigned to a sulfate anion. As evidence to support the binding of the substrate, prior to addition of 3PG to the model continuous density close to the sulfate/phosphate density was observed which could not be explained by either water molecules or sulfate anions. Subsequent refinement of the model with 3PG included improved the electron density surrounding the substrate and decreased R_{free}, indicating that the 3PG was favourably positioned. Refinement using a partial occupancy of 3PG in each active site was necessary because although the Michaelis constant for 3PG is 200 μM, competition with sulfate anions will occur as the crystal-growth conditions included ammonium sulfate in excess of 2 *M*. Refinement placing sulfate (occupancy 0.6) over the phosphate (occupancy 0.4) did not displace either molecule. A slight rotation of the sulfate moiety was observed, as expected, owing to the lack of constraint by the three-carbon sugar group. The *B* factors of the sulfate and 3PG are comparable with those of the nearby main-chain *B* factors (see Table 3). The difference maps clearly indicate that 3PG occupies an almost identical position in the active sites of both subunits at the base

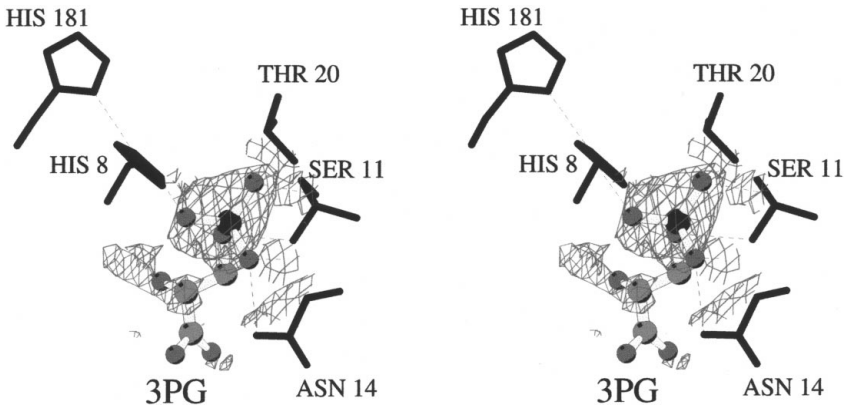

Figure 3
Stereo diagram showing the $F_o - F_c$ electron density calculated with 0.84 electrons per Å^3 for the 3PG substrate. All 3PG atoms were given an occupancy of zero. Side chains of active-site residues are also shown (bold black lines). Figure drawn using *MOLSCRIPT* (Kraulis, 1991).

of a 12 × 9 Å cleft and parallel to Asn14, with which it forms hydrogen bonds (Table 4). C1 of the 3PG is within 3.5 Å of His8. Hydrogen bonds to Arg7 and Arg59 also act to hold 3PG in place. Fig. 4 shows the electron density surrounding 3PG after refinement. The short half-life of phosphorylated *Sc*PGM (Nairn *et al.*, 1995) explains why no phosphate group is observed covalently bonded to His8, making this the crystallographic structure of a catalytically incompetent *Sc*PGM. Sufficient volume exists between His8 and 3PG to accommodate the phosphate moiety in the active site in a favourable position for reaction with 3PG. It is also likely that reorientation of the 2,3-BPG intermediate in the active site (Fothergill-Gilmore & Watson, 1989) is a possibility, since sufficient volume, occupied in this structure by ordered water molecules, exists around the substrate to allow this to occur.

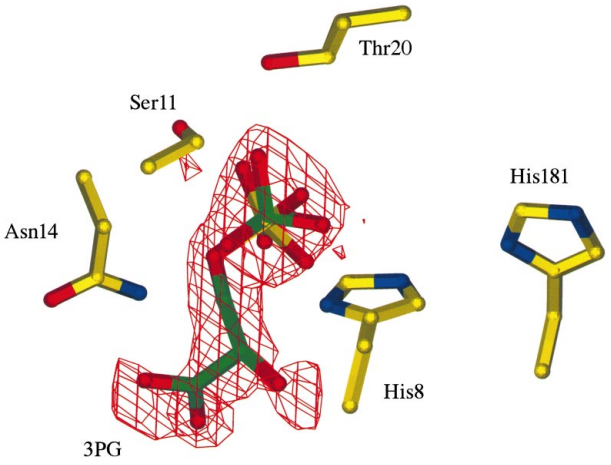

Figure 4
The $2F_o - Fc$ electron density (0.42 electrons per Å^3) surrounding the 3PG substrate after refinement. The sulfate anion is superimposed over the phosphate group. The 3PG and the sulfate have partial occupancies of 0.4 and 0.6, respectively. Figure drawn using *O-PLOT* (Jones *et al.*, 1991).

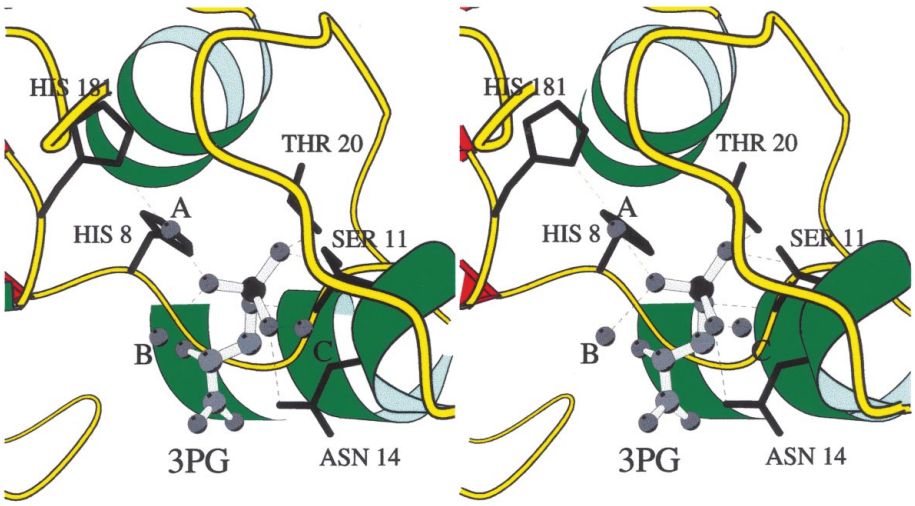

Figure 5
A stereo diagram showing secondary structure and hydrogen-bonding interactions (dashed lines) of 3PG within the *Sc*PGM active site with active-site residues (bold black lines) and ordered water molecules (grey spheres A, B and C). Figure drawn using *MOLSCRIPT* (Kraulis, 1991).

Table 4
Environment of sulfate anion and 3PG in subunit *A*.

Protein residue	Atom	Anion	Atom	Distance (Å)
Arg87	NH2	Sulfate†	O2	4.97
Lys97	NZ		O3	3.59
			O4	3.69
Arg113	NE		O4	2.59
	NH2		O4	2.99
Arg114	NH2		O1	4.78
	NE		O2	5.04
Arg7	NH2	3PG	O1	3.47
	NE		O3	3.49
Ser11	N		O1P	3.31
Asn14	N		O4P	3.81
	ND2		O2	3.60
			O1	3.73
Arg59	NE		O2P	2.78
His8	ND1		O3	3.64
	NE2		O2P	3.83

† As referred to in text.

3PG is held firmly in place by a network of hydrogen bonds from basic residues lining the active-site cleft to the phosphate-group and carbonyl-group O atoms as well as some hydrophobic interaction between Gln10 and the C3 of 3PG. The carbonyl group is also the most highly exposed to solvent at the entrance to the active site. Ordered water molecules with suitable *B* factors occupy part of the active site at distances of 2.7–3.3 Å from other possible hydrogen-bond donors/acceptors. The network of hydrogen bonds formed by these water molecules (Fig. 5) and active-site residues Ser11, Asn14 and Thr20 aid in positioning of the substrate.

The presence of bound 3PG does not appear to induce significant alterations in the structure of the active site of *Sc*PGM when compared with the native 2.3 Å structure. Several potential hydrogen-bond donors/acceptor side chains appear to have adopted slightly different orientations. The most recently published phosphoglycerate mutase structure (Rigden *et al.*, 1999) describes the presence of two sulfate anions in the active site, one of which (S1) appears to correspond to the phosphate moiety of bound 3PG in *Sc*PGM. The binding of the 3PG substrate would, therefore, appear to prevent the binding of a sulfate in this position. The second sulfate anion described here occupies a slightly different position to the S2 sulfate anion described by Rigden *et al.* (1999). The hydrogen-bonding distances holding this sulfate in place are described in Table 4. It is probable that the binding pattern of this second sulfate is altered by the presence of bound substrate. His8 and His181 are very slightly rotated about the $C_\beta - C_\gamma$ bonds; however, the positions of these catalytically important residues alter very little and probably do not signif-

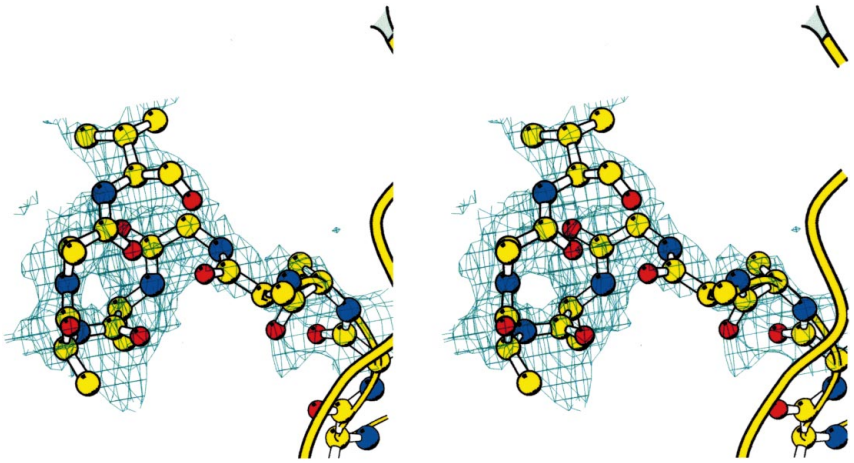

Figure 6
Stereo diagram showing residues *B*234 (right) to *B*240 (left) of the C-terminal tail with $2F_o - F_c$ electron density (0.3 electrons per Å^3) covering residues *B*236 to *B*240. C atoms are shown in yellow, N atoms in blue and O atoms in red. Figure drawn using *MOLSCRIPT* (Kraulis, 1991).

icantly alter hydrogen-bonding patterns. It is difficult to ascertain whether these changes are a consequence of the presence of the substrate affecting hydrogen-bonding networks or are simply because of the difference in resolution of the data collected.

The highly labile C-terminal amino acids beyond residues 234–235 were built into density close to the entrance to the active-site cleft (Fig. 6). Residues up to and including Val240 have been added to the model; however, further interpretation would have led to ambiguous results. The C-terminal tail partially covers the active site, confirming the theory that it constitutes a 'lid' or 'cap' to cover the active site during phosphate transfer. Interestingly, the main-chain O atom of Val240 is within hydrogen-bonding distance of the catalytically important Arg113. In this structure, the initial part of this C-terminal tail can be seen; however, the electron density becomes uninterpretable after residue 240 in each subunit and there is no unassigned density present in or on the model to suggest an 'anchor site' for any residues from 240 to 246. The exposed carbonyl group of 3PG probably forms hydrogen bonds to the mobile C-terminal region to stabilize the 'cap' formation.

Also of interest in the active site is the hydrogen-bond system Gly9 O···His181 ND1, His181 NE2···His8 NE2, His8 ND1···Ser55 OG, with hydrogen bonds of lengths 2.84, 2.79 and 2.86 Å, respectively. This system could act as a charge-transfer unit integral to the catalytic reaction and can be assumed to be in a conformation which would allow re-phosphorylation of His8 and, therefore, the reactivation of the enzyme. This observed system may be a rigid conformation which prevents the two His side chains from flexing, as there is certainly ample volume for movement of both side chains. The presence of a phosphate group attached covalently to His8 would probably disrupt this conformation.

Although the native *Sc*PGM structure (Rigden *et al.*, 1998) crystallized from a slightly different space group, it superimposes well (r.m.s.d. of 0.4) with the *Sc*PGM–3PG complex. This lack of observable conformational change of the active-site cleft on substrate binding suggests strongly that most crucial conformational changes involve the labile C-terminal region. The substrate-binding information provided in this structure should enable the design and modelling into the active site of inhibitors and putative drugs. The high-resolution positioning of active-site components should also help facilitate the interpretation of kinetic experiments which have been carried out to date. Coordinates of the ScPGM–3PG complex have been deposited with the Protein Data Bank.

Dr A. Rawas is acknowledged for his assistance with data collection. The initial data processing and refinement of this data was carried out by the late Dr H. C. Watson prior to his death in 1994. GSC is funded by a BBSRC studentship.

References

Allen, F. H. (1998). *Acta Cryst.* A**54**, 758–771.
Bernstein, F. C., Koetzle, T. F., Williams, G. J. B., Meyer E. F. Jr, Brice, M. D., Rogers, J. K., Kennard, O., Shimanouchi, T. & Tasumi, M. (1977). *J. Mol. Biol.* **112**, 535–542.
Brünger, A. T. (1992). *Nature (London)*, **355**, 472–474.
Campbell, J. W., Watson, H. C. & Hodgson, G. I. (1974). *Nature (London)*, **250**, 301–303.
Fothergill-Gilmore, L. A. & Watson, H. C. (1989). *Adv. Enzymol. Relat. Areas Mol. Biol.* **62**, 227–313.
Garel, M. C., Joulin, V., Le Boulch, P., Calvin, M. C., Prehu, M. O., Arous, N., Longin, R., Rosa, R., Rosa, J. & Cohen-Solal, M. (1989). *J. Biol. Chem.* **264**, 18966–18972.
Jones, T. A., Zou, J. Y., Cowan, S. & Kjeldgaard, M. (1991). *Acta Cryst.* A**47**, 110–119.
Kraulis, P. J. (1991). *J. Appl. Cryst.* **24**, 946–950.
Lamzin, V. S. & Wilson, K. S. (1993). *Acta Cryst.* D**49**, 129–147.
Laskowski, R. A., MacArthur, M. W., Moss, D. S. & Thornton, J. M. (1993). *J. Appl. Cryst.* **26**, 283–291.
Murshudov, G. N., Vagin, A. A. & Dodson, E. J. (1997). *Acta Cryst.* D**53**, 240–255.
Nairn, J., Krell, T., Coggins, J. R., Pitt, A. R. & Fothergill-Gilmore, L. A. (1995). *FEBS Lett.* **359**, 192–194.
Otwinowski, Z. & Minor, W. (1997). *Methods Enzymol.* **276**, 307–326.
Ravel, P., Croisille, L., Craescu, C. T., Rosa, J., Rosa, R. & Garel, M. C. (1996). *Br. J. Haematol.* **93**, 717.
Rigden, D. J., Alexeev, D., Phillips, S. E. V. & Fothergill-Gilmore, L. A. (1998). *J. Mol. Biol.* **276**, 449–459.
Rigden, D. J., Walter, R. A., Phillips, S. E. V. & Fothergill-Gilmore, L. A. (1999). *J. Mol. Biol.* **286**, 1507–1517.
Vagin, A., Murshudov, G. & Strokopytov, B. (1998). *J. Appl. Cryst.* **31**, 98–102.
Vaguine, A. A., Richelle, J. & Wodak, S. J. (1999). *Acta Cryst.* D**55**, 191–205.
White, M. F. & Fothergill-Gilmore, L. A. (1992). *Eur. J. Biochem.* **207**, 709–714.
Winn, S. I., Watson, H. C., Harkins, R. N. & Fothergill, L. A. (1981). *Philos. Trans. R. Soc. London*, **293**, 121–130.